

THE EFFECT OF SCATTERED RADIATION ON CAPABILITIES OF LASER BEAM GUIDANCE

Gennady A. Kaloshin¹, Vladimir P. Budak², Sergey A. Shishkin^{1,3},
and Vladislav V. Zhukov⁴

¹*V. E. Zuev Atmospheric Optics Institute of the Siberian Branch
of the Russian Academy of Sciences, Tomsk*

²*NIU MEI, Moscow*

³*JSC «Research Institute «Ekran», Samara*

⁴*Tomsk Polytechnic University, Tomsk*

E-mails: ¹gkaloshin@iao.ru

ABSTRACT

The paper discusses the possibility of remote detection of a continuous laser beam propagating in a scattering continental and coastal atmosphere, when it is recorded outside the axial zone. In the single scattering approximation, estimates of the radiance at the registration site are carried out, which are compared with the threshold characteristics of existing photodetectors in the visible and IR spectral regions. It is shown that the laser radiation (LR) of the beam is reliably recorded in the range of angles (0–180)° at metrological range of visibility equal (5–20) km at night conditions. At twilight, under the same conditions, detection capabilities are significantly reduced.

A significant increase of the LR beam radiance contrast with a decrease in its divergence has been shown experimentally in the field observations.

At twilight, a decrease in the beam's radiance contrast is seen. A beam with a divergence equal to 2' ceases to be distinguishable at angles equal to (80–90)°, and a beam with a divergence of 4' – at angles (60–70)°. In this case, the contrast difference reaches up to 10 times.

Keywords: aerosol scattering, indicatrices, contrast transfer, laser beam, photometer, continental and coastal atmosphere

INTRODUCTION

Many of applications in the fields of sensing, communication, and monitoring are performed by active and passive optical locator stations (OLS). They use powerful sources of laser radiation (LR) with propagation distance of several kilometres in the most dynamic part of the atmosphere: surface air. It is desirable to know the location and direction of a LR beam. In [1–5], it is shown that LR is detectable due to scattering by aerosols and a beam may be displayed by photodetectors (PD). It follows from these works that intensity of LR scattering is corresponds to the prediction based on Mie scattering [6–9] for coastal and continental aerosols. It is known that concentration of aerosol varies significantly depending on regional and local weather conditions [10–13]. For example, increased moisture increases concentration of aerosols and, typically, scattering of LR [14–18]. In typical conditions (mist, thin fog, etc.), even at low altitude, scattering is slight and hardly detectable if there is a background. This poses special requirements, on the one hand, on the PD characteristics: sensitivity, response time, and spectral responsivity range, and, on the other hand, on information about the optical properties of the atmosphere and mostly the aerosol as the main component affecting the attenuation and scattering of LR in atmospheric transparency windows

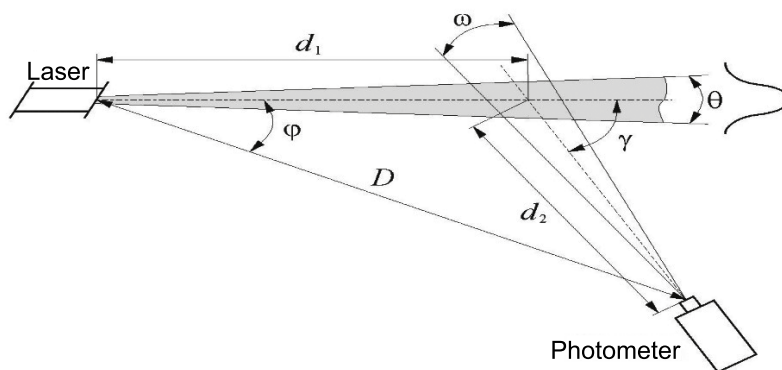


Fig. 1. Diagram of scattered laser radiation detection

[19, 20]. Despite the fact that there are different methods of predicting signal variations at entrance pupils of OLS, it is necessary to further enhance the existing methods and approaches and to develop new methods of remote detection of LR in real operating conditions. This is due to both the development of LR sources and PD's [21–23] and enhancement of aerosol models of surface air [24–27].

The main goals of this work are the study of off-axis detection of LR and measurement of LR radiance contrast, including during field measurements.

The goal of the work is to study patterns of aerosol scattering when estimating capabilities of off-axis detection of LR in continental and near-coast conditions in case of changes of beam parameters, meteorological visibility (MV), time of the day, and distances to LR source.

The work included theoretical evaluations of one-time scattered radiation based on the *MaexPro* aerosol model [28, 29], where sea salt consists of water droplets and salt particles, and aerosol of continental haze with particles radii (0.01–100) μm as the most optically active in wavelength band ORS of (0.2–12) μm . For the following basic conditions of numerical calculations: height above sea level $H = (0\text{--}25)$ m; wind speed $U = (3\text{--}18)$ m/s; wind speed $U = (3\text{--}18)$ m/s; The rest of the conditions are given in the text at the place of mention. In the calculations, we used computer programs [30–33], as well as a program for experimental estimates of the intensity contrast of LR in field conditions [34].

1. RESULTS OF CALCULATIONS

Radiance of scattered LR in surface air is selected as the main magnitude allowing to specifically evaluate capabilities of off-axis detection of a laser beam. Contemporary photometers (spectroradiometers)

allow to confidently detect superweak signals within the spectral range of (0.35–1.1) μm by means of non-cooled silicon photodiode detectors and photomultipliers within the spectral range of (0.35–0.93) μm with responsivity thresholds at level of 3σ (depreciation factor is 6) ($3 \cdot 10^{-10}$) W/nm and ($3 \cdot 10^{-14}$) W/nm, respectively. These spectroradiometers manufactured by instrument systems [35] have threshold responsivity of (10^{-6} – 10^{-7}) lx within the spectral range of (0.2–5) μm , which allows to register the background of moonless starry sky at ($3 \cdot 10^{-4}$) lx or, for example, light of Sirius at 10^{-5} lx. For cooled photomultipliers operating within spectral range of (0.35–0.93) μm with *GaAs* photocathode, noise equivalent power equals to 10^{-13} W/($\text{cm}^2 \cdot \text{sr} \cdot \text{nm}$) and luminance responsivity is of approximately 10^{-3} cd/m².

The work considers the model of off-axis scattering of LR for optimizing the detector characteristics and predicting the luminous efficacy of its operation in coastal areas when moving the optical axis of a PD perpendicular to and along the beam axis along a horizontal path in night and twilight conditions with different VS.

The diagram of the numerical experiment for the two-dimensional case to determine the distance of off-axis detection of continuous LR passing through a scattering environment is shown in Fig. 1. The Gaussian LR beam with wavelength of λ , initial power of P_0 , and divergence of θ at the level of 0.5 is directed in parallel to the earth's surface in direction φ relative to the PD. PD is located at distance D from the source of LR with angle of view ω . Scattered LR is seen at angle of γ .

The distances D and d_2 at which the condition $L/L_t \geq 1$ where L_t is the threshold radiance for a specific PD is met, for LR scattered towards the radiance PD L , are taken as distance of off-axis detection.

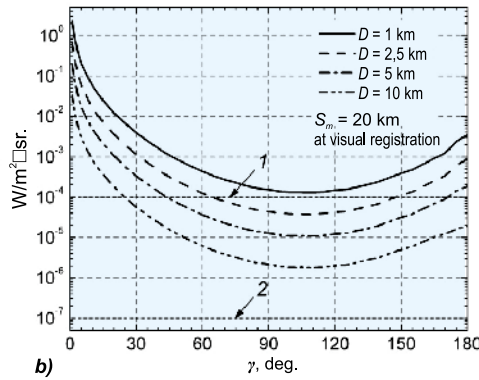
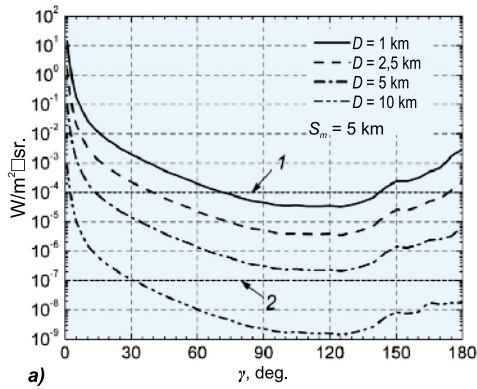


Fig. 2. Change of radiance of a laser beam L by $\lambda = 0.52 \mu\text{m}$ at $P_0 = 1 \text{ W}$ and $\theta = 3'$ depending on scattering angle γ in the course of scanning of PD field-of-view axis along the beam axis with different distances D from the emitter with $S_m = 5 \text{ km}$ (a) and $S_m = 20 \text{ km}$ (b)

L was calculated for one-time scattering, which is reasonable for small optical thicknesses when solving atmospheric problems [17]. Molecular scattering was assumed to be low.

L at the cross-section with the PD field of view axis was calculated as

$$L = \frac{10^{-3}}{4\pi} \cdot \frac{\chi(\gamma) \cdot \exp[-\sigma(\lambda) \cdot d_2 \cdot 10^{-3}]}{\sin \gamma} \int_{-R}^R E(r) dr, \quad (1)$$

where $\sigma(\lambda)$ is spectral coefficient of aerosol scattering, λ is LR wavelength, $\chi(\gamma)$ is directional aerosol light scattering coefficient, γ is scattering angle; d_2 is distance between PD and the sight point at the beam axis, $E(r)$ is irradiance formed by the laser beam at the given point, r is beam radius in a plane of the sight point.

$E(r)$ was defined using the formula

$$E(r) = \frac{2P_0}{\pi \cdot r^2} \cdot \exp(-\sigma(\lambda) \cdot d_1 \cdot 10^{-3}) \cdot \exp\left(-2\frac{r^2}{r_0^2}\right), \quad (2)$$

where P_0 is LR power at entrance of the environment, d_1 is the distance between the laser and the point of sight, $r_0 = r_0 + d_1 \cdot \text{tg}(\theta/2)$ is the beam radius at divergence level θ in the plane of the sight point,

r_0 is the beam radius at aperture exit, θ is beam divergence at level of 0.5 rad; $R = d_2 \cdot \text{tg}(\omega/2)$ is the distance across the beam limited by the PD field of view; ω is the vision angle of PD.

Using the eqs. (1) and (2), the values of L were calculated for coastal mist with MV S_m of 5 km and 20 km with different geometry of the detection scheme (D, φ) and scattering angles γ in range (0–180)°. The obtained values were compared with threshold radiance responsivity of the selected PD's (for evaluation of the distance of off-axis detection). The following values of LR beam parameters were taken as $P_0 = 1 \text{ W}$, $\lambda = 0.52 \mu\text{m}$ and $1.06 \mu\text{m}$, $\theta = 3'$, and $r_0 = 2 \text{ mm}$. The factors $\sigma(\lambda)$ and $\chi(\gamma)$ were calculated using the data of the *MaexPro* model [28, 29]. For example, at $\lambda = 0.52 \mu\text{m}$ and $S_m = 5 \text{ km}$ and 20 km, $\sigma = 0.83 \text{ km}^{-1}$ and 0.75 km^{-1} , respectively, and at $\lambda = 1.06 \mu\text{m}$, it equals to 0.21 km^{-1} and 0.11 km^{-1} , respectively. Some values of the factors $\chi(\gamma)$ (at $\gamma = 1^\circ, 3^\circ, 5^\circ, 45^\circ, 90^\circ$ and 135°) are given in Table 1.

The threshold responsivity of PD was selected using the data of [35] with consideration of transformation of energy quantities into luminous quantities using spectral luminous efficacy $V(\lambda)$ at $\lambda = 0.52 \mu\text{m}$. The values of L_t at $\lambda = 0.52 \mu\text{m}$ for night and twilight conditions were equal to $10^{-7} \text{ W}/(\text{m}^2 \cdot \text{sr})$

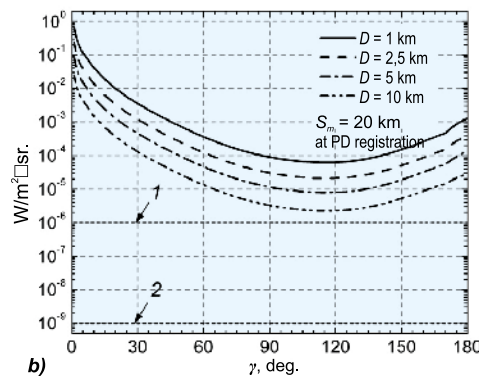
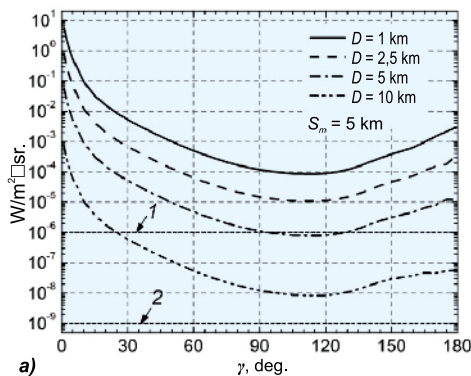


Fig. 3. Change of radiance of a laser beam L by $\lambda = 1.06 \mu\text{m}$ at $P_0 = 1 \text{ W}$ and $\theta = 3'$ depending on scattering angle γ in the course of scanning of PD field-of-view axis along the beam axis with different distances D from the emitter with $S_m = 5 \text{ km}$ (a) and $S_m = 20 \text{ km}$ (b)

Table 1. The Values (Selected) of the Coefficients $\chi(\gamma)$ Taken for Calculation

| $S_m, \text{ km}$ | $\lambda \text{ LR}, \mu\text{m}$ | $\chi(\gamma), \text{ km}^{-1} \cdot \text{sr}^{-1}$ | | | | | |
|-------------------|-----------------------------------|--|--------------------|--------------------|---------------------|---------------------|----------------------|
| | | $\gamma = 1^\circ$ | $\gamma = 3^\circ$ | $\gamma = 5^\circ$ | $\gamma = 45^\circ$ | $\gamma = 90^\circ$ | $\gamma = 135^\circ$ |
| 5 | 0.52 | 20 | 3.7 | 1.2 | 0.032 | 0.0038 | 0.0029 |
| | 1.06 | 8.1 | 6.2 | 3.8 | 0.087 | 0.0098 | 0.0092 |
| 20 | 0.52 | 6.7 | 4.5 | 3.0 | 0.13 | 0.026 | 0.025 |
| | 1.06 | 3.5 | 3.3 | 3.0 | 0.22 | 0.027 | 0.017 |

and $10^{-4} \text{ W}/(\text{m}^2 \cdot \text{sr})$, respectively, and at $\lambda = 1.06 \mu\text{m}$, they were equal to $10^{-9} \text{ W}/(\text{m}^2 \cdot \text{sr})$ and $10^{-6} \text{ W}/(\text{m}^2 \cdot \text{sr})$, respectively. The angle ω in this case was equal to 20° .

As an example, the Figs. 2 and 3 show the results of calculation of L depending on γ in the visible ($\lambda = 0.52 \mu\text{m}$) at visual registration and the near-IR ($\lambda = 1.06 \mu\text{m}$) regions of the spectre when scanning the PD axis along the axis of the beam at $S_m = 5 \text{ km}$ and 20 km and different values of D .

The calculation results show that the possibilities of detecting scattered LR in the visible range with visual registration at $S_m=20 \text{ km}$ (Fig. 2b) are higher than at $S_m=5 \text{ km}$ (Fig. 2a) for all scattering angles. This is explained by the greater attenuation due to scattering at lower S_m on particles of atmospheric haze (Mie particles). The threshold brightness levels in Fig. 2 are indicated by lines 1 and 2 for twilight and night conditions, respectively. In the near-IR range during PD registration with a decrease in the background level by two orders of magnitude to the values indicated in Fig. 3 by lines 1 and 2, the possibilities of detecting scattered LR beams are much higher. The figures show that at night conditions, at $S_m = 5 \text{ m}$, the LR beam will be detected at distance $D = 10 \text{ km}$ at $\gamma = 45^\circ$. At $\gamma = (110-120)^\circ$ (minimal values of L), the distance of detection D at $S_m = 5 \text{ km}$ reduces to 5 km , and at

$S_m = 20 \text{ km}$, the LR beam is confidently detected at D exceeding 10 km . In the twilight, at the same values of γ , capabilities of detection reduce significantly down to $D = 1 \text{ km}$ for both 5 km and 20 km .

2. RESULTS OF FIELD MEASUREMENTS

In 2015–2018, to confirm the results of the calculations, the field measurements were conducted in night and twilight conditions at the test area of the V.E. Zuev Atmospheric Optics Institute of the Siberian Branch of the Russian Academy of Sciences. During the measurements, the background luminance was $10^{-2} \text{ cd}/\text{m}^2$ (night) and $0.5 \text{ cd}/\text{m}^2$ (twilight), respectively. During the measurements, the sky was cloudy, and the Moon was below the horizon. MV varied within the range of (12–15) km.

2.1. Scheme of the Experimental Installation

The emitter model (Fig. 4) contained a semiconductor laser *DTL-313* ($\lambda = 0.527 \mu\text{m}$, $P_0 = 117 \text{ mW}$, $\theta = 1 \text{ mrad}$, $d_0 = 2 \text{ mm}$) and the telescopic beam collimation system for adjustment of θ . To measure L , *LS-110* PD by *Konica Minolta* was used (the range of luminance measurements of (0.01–999,

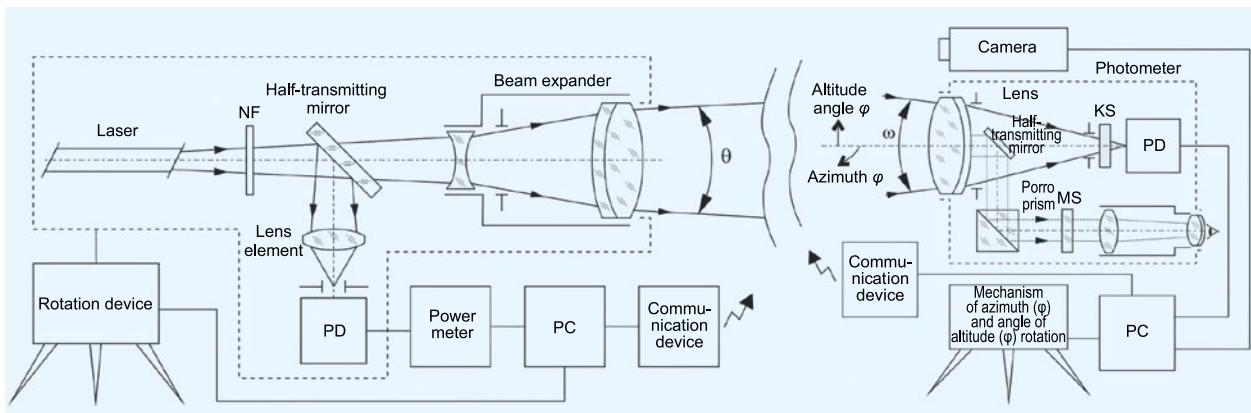


Fig. 4. Diagram of the experimental installation for measurement of luminance of scattered laser radiation

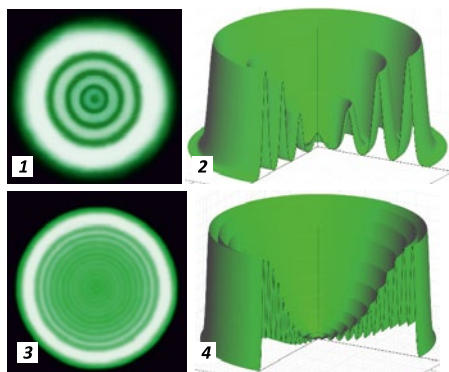


Fig. 5. Cross-sectional distribution of luminance of laser radiation beams in the form of 4 and 12 concentric rings (photos 1 and 3 respectively) and the results of photometry of the same beams (2 and 4)

900) cd/m^2 , $\omega = 1/3^\circ$) with a Canon EOS6D camera (resolution of 20 Mpx (megapixels), EF (24–105) mm lens, $f/4L$). The equipment was installed on a rotating platform to move along the azimuth and angle of altitude. The measurement data was registered by a PC and processed by means of the developed software [36, 37].

The measurements were conducted following the scheme shown in Fig. 1. The directional light scattering coefficient γ was registered in the range of angles of $\gamma = (0.5–179.5)^\circ$ with a step of 5° at the set values of D and φ . Due to structural features, the PD did not reach the border values of γ at 0.5° . The beam passed at altitude of about 2 m above the earth surface. Before commencement of measurement, a standard pegging-out of the area was conducted to define the parameters of the LR path and

to define the places of PD installation so that their optical axes were in one plane and crossed each other.

The structure of laser beams used for measurements is shown in Fig. 5.

Recently, LR beams with circular structure of intensity distribution, which may be well approximated cross-sectionally by the Gaussian function are of interest. Fig. 5 shows that the external ring of both types of beams has the highest radiance, which reduced to the centre of the beam according to the law close to the Gaussian distribution. The main power of the beam is concentrated in the first two rings. In Fig. 5, white colour depicts maximum intensity and black colour depicts zero intensity. Here, cross-sectional distribution of intensity is presented as concentric 4 rings and 12 rings with $\theta = 2'$ и $4'$, respectively.

An example of an image of beams shot from one side is shown in Fig. 6. The geometry of the detection scheme was as follows: $D = 150$ m, $\varphi = 2^\circ$, $\gamma = 45^\circ$.

2.2. Results of Measurement of LR Beam Luminance Contrast

The measured luminance of LR beams in direction perpendicular to their axis is shown in Fig. 7 at two values of angular detection directions $\gamma = 45^\circ$ and 90° . In the shot of the LR beams (Fig. 6), the detector axis was located near the centre of the image along the axis of a respective beam.



Fig. 6. The image of laser radiation beams ($\lambda = 0.527 \mu\text{m}$, $P_0 = 117$ mW), side view, on a near-surface path, with beam divergence $\theta = 2'$ (a) and $4'$ (b)

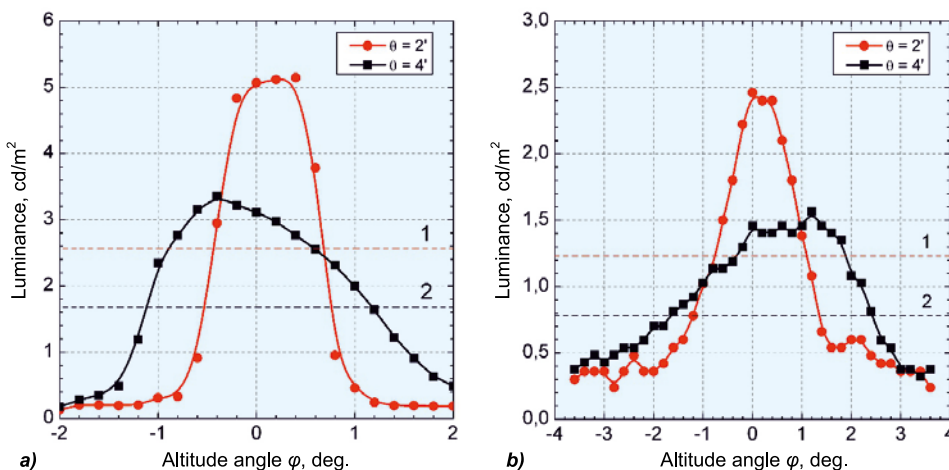


Fig. 7. Change of luminance of the laser radiation beams ($\lambda = 0.527 \mu\text{m}$, $P_0 = 117$ mW) with divergence of $\theta = 2'$ and $4'$ when displacing the field-of-view axis of the photometer perpendicular to the beam axis at acceptance angles $\gamma = 45^\circ$ (a) and 90° (b)

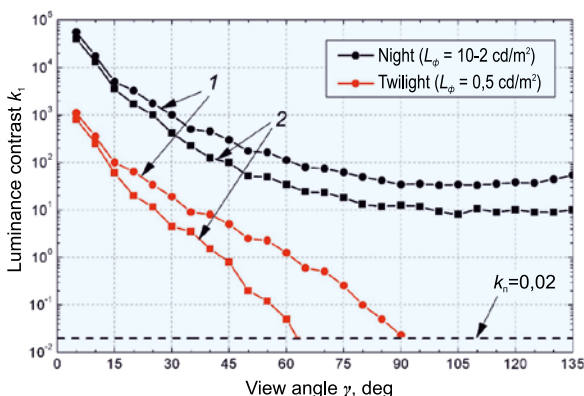


Fig. 8. Change of luminance contrast k of the laser beam ($\lambda = 0.527 \mu\text{m}$, $P_0 = 117 \text{ mW}$) with divergence of $\theta = 2'$ (curves 1) and $4'$ (curves 2) at night and twilight conditions when the field-of-view axis of the photometer is displaced angularly along the beam axis

The capability of guidance along the LR beam was evaluated by the value of luminance contrast k defined using the expression

$$k = (L_0 - L_b) / L_b, \tag{3}$$

where L_0 is luminance of the scattered LR beam; L_b is background luminance. At $k \rightarrow 1$, the observed LR beam is extremely contrast, and the case of $k \rightarrow 0$ corresponds to complete scattering of the LR beam. For definition of k of the LR beam, the value of the beam luminance L_0 was selected on the level of $0.5 \cdot L_{\text{max}}$ depicted by horizontal lines 1 (at $\theta = 2'$) and 2 (at $\theta = 4'$) in Fig. 7. At $\gamma = 45^\circ$, the values of k calculated using (3) were equal to 0.51 and 0.33 for LR beams with $\theta = 2'$ и $4'$, respectively. At $\gamma = 90^\circ$, $k = 0.33$ for the LR beam with $\theta = 2'$ and $k = 0.12$ for the LR beam with $\theta = 4'$. Therefore, Fig. 7 illustrates a significant reduction of k of the beam with increasing θ .

To evaluate the detection capabilities of the LR beam, several series of the beam k were measured at different values of γ depending on background observation conditions. The measured background luminance L_b was equal to about 10^{-2} cd/m^2 and 0.5 cd/m^2 for the night and twilight conditions, respectively. The selected detection scheme was as follows: $D = 1200 \text{ m}$, $\varphi = 5^\circ$, $\gamma = (5-135)^\circ$.

Changes in k of the LR beams at $\theta = 2'$ и $4'$ are shown in Fig. 8. The horizontal line here depicts the level of threshold luminance contrast k_t , which was selected equal to 0.02 as per the recommendations [38, 39] for approximate calculations.

3. DISCUSSION OF THE RESULTS

The results show (Fig. 7) that k of LR beams significantly reduces with increase of θ . This is caused by an increase in background radiation due to multiple scattering of the beam itself. Moreover, it follows from Fig. 8 that k of LR beams at night conditions is much higher than k_t within the entire range of angles γ , which confirms that they are found reliably. The initial sections of the beams up to $(15-20)^\circ$ are especially contrast and were also perceived visually the same in both beams. With increase of the angles γ , the beam with $\theta = 2'$ was seen more contrast, and its k was (3–5) times higher than that of the beam with $\theta = 4'$.

At twilight conditions, a significant decrease in k of both beams was seen. The beam with $\theta = 2'$ becomes not detectable at $(80-90)^\circ$, and the beam with $\theta = 4'$ becomes not detectable at $(60-70)^\circ$. In this case, the difference between the values of k becomes 10-fold.

4. CONCLUSIONS

The results of the calculations and field measurements show that the values of k of the selected types of LR beams strongly depend on θ and S_m .

It is demonstrated that LR is reliably detected within the range of angles of $(0-180)^\circ$ at $(5-20) \text{ km}$ at night and twilight conditions with background luminance of 10^{-2} cd/m^2 and 0.5 cd/m^2 , respectively.

Field experiments have showed that k of the LR beam significantly reduces with decrease of its θ . In twilight conditions, significant reduction of k of both beams was seen. The beam with $\theta = 2'$ becomes not detectable at $(80-90)^\circ$, and the beam with $\theta = 4'$ becomes not detectable at $(60-70)^\circ$. In this case, the difference between the values of k ultimately becomes 10-fold.

ACKNOWLEDGEMENT

The work was conducted with financial support of the Ministry of Science and Higher Education of the Russian Federation.

REFERENCES:

1. Roy N., Reid F. Off-axis laser detection model in coastal areas, Optical Engineering, 2008. V47, pp. 1–11.

2. Cariou J.P. Off-axis detection of pulsed laser beams: simulation and measurements in the lower atmosphere, Proceedings of SPIE, 2003. V5086, pp. 129–138.
3. Michulec J. K., Schleijsen R. Influence of aerosols on off-axis laser detection capabilities, Proceedings of SPIE, 2009. V7463, pp. 1–12.
4. DeGrassie John S. Modeling off-axis laser scattering: effects from aerosol distributions, Proceedings of SPIE, 2012. V8517 (85170V).
5. Mendoza-Yero, O. Effects of off-axis laser beam propagation on beam parameters, Proceedings of SPIE, 2014. V5622.
6. Kaloshin G.A., Piazzola J. Influence of the large aerosol particles on the infrared propagation in coastal areas, Proceedings of 23rd International Laser Radar Conference, 2006. pp. 429–432.
7. Kaloshin G.A., Piazzola J., Shishkin S. Numerical modeling of influence of meteorological parameters on aerosol extinction in the marine atmospheric surface layer, Proceedings of 16th International Conference on Nucleation and Atmospheric Aerosols (ICNAA), 2004. p. 352–354.
8. Kaloshin G.A. Modeling the Aerosol Extinction in Marine and Coastal Areas, IEEE Geoscience and Remote Sensing Letters, 2020, april. URL: <https://ieeexplore.ieee.org/document/9052468> (date of reference: 20.06.2020); doi: 10.1109/LGRS.2020.2980866.
9. Kaloshin G.A. Method of Building of a Visual Landing-and-Takeoff System by Means of Vortex Laser Beams, Patent of Russia No. 2695044, 2018. V32.
10. Gathman S.G. Optical properties of the marine aerosol as predicted by the Navy aerosol model, Optical Engineering, 1983. V22, #1, pp. 57–62.
11. Gathman S.G. J. van Eijk A.M. and Cohen L.H. Characterizing large aerosols in the lowest levels of the marine atmosphere, Proceedings of SPIE, 1998. V3433, pp. 41–52.
12. Shettle E.P. Models of aerosols clouds and precipitation for atmospheric propagation studies, Proceedings of AGARD Conference: Atmospheric Propagation in the UV Visible IR and MM-Wave region and Related Systems Aspects, 1989. V454, pp. 15–1 – 15–13.
13. Weichel H. (ed.) Laser Beam Propagation in the Atmosphere. – SPIE Bellingham WA. – 28.09.1990.
14. Zuev V.E. Propagation of Visible and Infra-Red Waves in Atmosphere [Rasprostranenie vidimyykh i infrakrasnykh voln v atmosfere]. – Moscow: Sovetskoye radio, 1970. 496 p.
15. Zuev V.E. Propagation of Laser Radiation in Atmosphere [Rasprostranenie lazernogo izlucheniya v atmosfere]. Moscow: Radio i svyaz, 1981. 288 p.
16. Zuev V.E., Krekov G.M. Optical Models of Atmosphere [Opticheskiye modeli atmosfery]. – Leningrad: Gidrometeoizdat, 1986. 256 p.
17. Zuev V.E., Kabanov M.V., Saveliev B.A. Propagation of Laser Beams in a Scattering Environment [Rasprostranenie lazernyykh puchkov v rasseivayushchey srede], Applied Optics, 1969. V8, #1, pp. 137–141.
18. Deymerdjan D. Scattering of Electromagnetic Radiation by Spherical Polydisperse Particles [Rasseyaniye elektromagnitnogo izlucheniya sfericheskimi polidispersnyimi chastitsami]. – Moscow: Mir, 1971. 290 p.
19. Jensen D.R., Gathman S.G., Zeisse C.R., Littfin K.M. EOPACE overview and initial accomplishment, Journal of Aerosol Science, 1999. V30, #1, pp. 53–54.
20. Jensen D.R., Gathman S.G., Zeisse C.R., Leeuw G., de Smith M.H., Frederickson P.A., Davidson K.L. Electrooptical Propagation Assessment in Coastal Environments (EOPACE): summary and accomplishments, Optical Engineering, 2001. V40, #8, pp. 1486–1498.
21. Kaloshin G.A., Gordienko A.I. Laser aids to navigation (methods), IALA Bulletin. 2003. V3, pp. 46–51.
22. Kaloshin G.A. Gordienko A.I. Laser aids to navigation (technologies), IALA Bulletin, 2004. #1, pp. 42–49.
23. Gordienko A.I. Kaloshin G.A. Laser leading beacons: summaries and perspectives, Proceedings of XV Conference IALA “Navigation and the Environment”, 2002. pp. 150–158.
24. Jensen D.R. Gathman S.G. Zeisse C.R. and Littfin K.M. EOPACE (Electrooptical Propagation Assessment in Coastal Environments) Overview and Initial Accomplishments /Proceedings of Millennium Conference on Antennas and Propagation (AP2000). – Davos Switzerland, 2000.
25. Nilsson B.A. Meteorological influence on aerosol extinction in the 0.2–40 μ wavelength range, Applied Optics, 1979. V18, pp. 3457–3472.
26. Nilsson B.A. Model of the relation of IR aerosol extinction to weather parameters, Proceedings of SPIE: Infrared Technology XVIII, 1992. V1762, pp. 238–250.
27. Lewis E.R., Schwartz S.E. Sea salt aerosol production: Mechanisms methods measurements and models – a critical review. Geophys. Monograph. Washington DC: AGU, 2004. 413 p.
28. Kaloshin G.A., Grishin I.A. An aerosol model of the marine and coastal atmospheric surface layer, Atmosphere, Ocean, 2011. V49, #2, pp. 112–120.
29. Kaloshin G.A. Development of the Aerosol Model of the Near-Earth Layer of Marine and Coastal Atmosphere [Razvitiye aerolnoy modeli prizemnogo sloya morskoy i pribrezhnoy atmosfery]. Optika atmosfery i okeana, 2018. V31, #11, pp. 881–887.
30. Kaloshin G.A., Shishkin S.A. The Range Software Package for Calculations of Optical Radiation Propagation with Consideration of Aerosol Attenuation in the Near-Surface Layer of the Continental Marine and Coastal Atmosphere [Programmno-tekhnologicheskii paket

Range dlya provedeniya raschyotov rasprostraneniya opticheskogo izlucheniya s uchyotom aerolnogo oslableniya v prizemnom sloye kontinentalnoy morskoy i pribrezhnoy atmosfery], Certificate of State Registration of Computer Software No. 2012616944 dated on 08/03/2012.

31. Kaloshin G.A., Shishkin S.A. MaexPro Software Package for Calculation of Spectral Aerosol Attenuation Coefficients in the Near-Surface Layer of Marine and Coastal Atmosphere [Programma dlya raschyota spektralnykh koeffitsientov aerolnogo oslableniya v prizemnom sloye morskoy i pribrezhnoy atmosfery MaexPro] / Certificate of State Registration of Computer Software No. 2012616945 dated 08/03/2012.

32. Kaloshin G.A., Shishkin S.A. MieCalc Software Package for Calculation of Complex Refractive Indices of a Material of Marine and Coastal Aerosol Particles [Programma dlya raschyota kompleksnykh pokazateley prelomleniya veshchestva chatits morskogo i pribrezhnogo aerolya MieCalc]. Certificate of State Registration of Computer Software No. 2012616943 dated 08/03/2012.

33. Kaloshin G.A., Shishkin S.A. Zhukov V.V. Microphysical and Optical Characteristics of Marine and Coastal Aerosol [Mikrofizicheskiye i opticheskiye kharakteristiki morskogo i pribrezhnogo aerolya]. Certificate of State Registration of a Database No. 2015621775 dated 12/14/2015.

34. Kaloshin G.A., Shishkin S.A. Zhukov V.V. Characteristics of scattered radiation in off-axis recording of laser radiation under field conditions, Proceedings of SPIE 25th Intern. Symp. on Atmospheric and Ocean Optics: Atmospheric Physics, 2019. V11208, P. 112081C.

35. Instrument Systems. URL: <http://www.instrumentsystems.com/> (date of reference: 20.06.2020).

36. Kaloshin G.A., Shishkin S.A., Zhukov V.V. Software Package for Control and Processing of the Data of Spectroradiometry Measurements of Scattered Radiation of Laser Beams in Atmosphere [Programma dlya upravleniya i obrabotki dannykh spektrometricheskikh izmereniy resseyannogo izlucheniya lazernykh puchkov v atmosfere] / Certificate of State Registration of Computer Software No. 2015618954 dated 08/20/2015.

37. Kaloshin G.A., Shishkin S.A., Zhukov V.V. Software for Control of Measurements of Laser Beam Luminance Contrast in Scattering Environments [Programma upravleniya izmereniyami kontrasta yarkosti lazernykh puchkov v rasseivayushchikh sredakh] Certificate of State Registration of Computer Software No. 2015663204 dated 12/14/2015.

38. Meshkov V.V., Matveev A.B. Basics of Light Engineering: Study Guide for Higher Education Institutions: in 2 parts. P. 2. Physiological Optics and Colourimetry [Osnovy svetotekhniki: uchebnoye posobiye dlya vuzov: v 2 ch. Ch. 2. Fiziologicheskaya optika i kolorimetriya].

2nd edition, revised and supplemented. Moscow: Energoatomizdat, 1989, 432 p.

39. Luizov A.V. Eye and Light [Glaz i svet]. – Leningrad: Energoatomizdat, Leningrad Branch, 1983. 144 p.



Gennady A. Kaloshin, Ph.D (phys.-math.) He graduated from Tomsk State University with specialty in Radiophysics and Quantum Electronics in 1972. Leading Scientist

Researcher of V.E. Zuev Atmospheric Optics Institute of the Siberian Branch of the Russian Academy of Sciences



Vladimir P. Budak, Professor, Doctor of Technical Sciences. In 1981, he graduated from the Moscow Power Engineering Institute (MPEI). At present, he is the Editor-in-chief of the Svetotekhnika /

Light & Engineering journal, Professor of the Light Engineering sub-department of NRU MPEI. Corresponding member of the Academy of Electrotechnical Sciences of Russia



Sergey A. Shishkin is Leading engineer, Head of department. He graduated from Tomsk University of Control Systems and Radioelectronics in 2000. He works at Joint Stock Company “Research

Institute “Ekran”, Samara and V.E. Zuev Institute of Atmospheric Optics SB RAS



Vladislav V. Zhukov graduated from Tomsk Polytechnic University, Tomsk. Now he is engineer at Tomsk Polytechnic University